SPURIOUS REFLECTIONS IN FINITE/INFINITE ELEMENT MESHES
(IN PROGRESS: 1. THE ONE-DIMENSIONAL CASE)

Francisco Medina and Fernando Rosales

Facultad de Ciencias Físicas y Matemáticas
Universidad de Chile
Casilla 2777, Santiago

ABSTRACT

When numerically analyzing unbounded wave propagation problems, spurious reflections arise from numerical reflections produced on the fictitious boundary of the discretization. If infinite elements model the far field of this class of problems, the finite-infinite element interfaces act as numerical scatters. Due to this effect, part of the energy carried by the outgoing waves is reflected, generating a source of error in the numerical solution. This study analyzes the spurious reflections arising from finite/infinite element discretizations. The ratios of wave amplitude and mean energy flux between the outgoing wave and the corresponding reflected and refracted waves are quantified. The results provide criteria for mesh design in order to diminish numerical noise coming from undesired boundary reflections.

RESUMEN

Al analizar numéricamente problemas de propagación de ondas, definidos en medios no acotados, existen reflexiones numéricas que se producen sobre el borde ficticio de la discretización. Si el campo lejano de este tipo de problemas se modela con elementos infinitos, las interfaces entre los elementos finitos y los infinitos actúan como pantallas numéricas. Debido a este efecto de pantalla, parte de la energía de la onda incidente se refleja, generando una fuente de error en la solución numérica. El presente trabajo analiza las reflexiones numéricas que se producen debido a discretizaciones de elementos finitos e infinitos. Se cuantifican las razones de amplitud de onda y flujo medio de energía, entre la onda incidente y las ondas reflejada y refractada. Los resultados aportan criterios para el diseño de mallas, que permiten disminuir los errores numéricos producidos por reflexiones indeseables sobre el borde.

INTRODUCTION

Since the first application[1] of infinite elements to solve unbounded domain problems, techniques using finite/infinite elements have appeared with increasing frequency in the literature. Among the many applications carried out with this technique, it has also been applied to problems involving wave propagation[2,3] and dynamic interaction.[4,5] By using infinite elements, it is possible to model the far field (ff) of unbounded media without loosing the flexibility of the classical finite element method. In effect, the near field (nf) modeled with finite elements may be nonhomogeneous and anisotropic. However, the treatment of transient problems presents some difficulties. Nevertheless, problems that are dynamic in nature have been successfully treated, but certain questions on the merits of the technique still remain.

As waves travel through a mesh, artificial reflections arise due to changes in the approximation of the discretization.[6,7] In the case of transient and wave propagation problems defined in unbounded domains, these phenomena have received insufficient attention in the literature. In this work, a study is presented to quantify the spurious reflections produced in the interface between nf and ff (far-field boundary, ffb). This formulation is restricted to unbounded media that can be geometrically modeled in one dimension, i.e., this formulation is restricted to cases of one-dimensional, cylindrically symmetric, and spherically symmetric wave propagation.

FORMULATION OF THE PROBLEM

The ffb is defined as the interface between the mesh of finite elements and the mesh of infinite elements. The latter have been developed to replace the ff and transmit the waves coming from the nf into the ff. However, due to the numerical approximation, the ffb acts as a scatter and reflects part of the incident waves. This is due to three factors: (a) there is a numerical discontinuity on the ffb, produced by the change of displacement approximation in the discretization; (b) the nf displacement approximation introduces errors; and (c) if the ff approximation is not derived from exact solutions to the problem considered, it leads to further errors. By studying the equilibrium and the wave propagation pattern on both sides of the ffb, the scattering effect can be quantified.

Equilibrium Equation.

Considering an elastic medium discretized by finite and infinite elements, as shown in Fig.1, the frequency-dependent dynamic equilibrium equation, for each element e and frequency ω, is given[8] by

$$\mathbf{K}^e(\omega)\mathbf{u}^e(\omega) \;=\; \mathbf{p}^e(\omega) \tag{1}$$

where $\mathbf{K}^e$ is the element dynamic stiffness matrix and, $\mathbf{u}^e$ and $\mathbf{p}^e$ contain the element nodal displacements and loads, respectively. In absence of external loads, the internal degrees of freedom for the finite element adjacent to the ffb, see Fig.2, can be condensed out from Eq.(1), yielding

$$\begin{bmatrix} k_{nn}^* & k_{n0}^* \\ k_{0n}^* & k_{00}^* \end{bmatrix}^e \begin{bmatrix} u_n \\ u_0 \end{bmatrix}^e \;=\; \begin{bmatrix} p_n \\ p_0 \end{bmatrix}^e \tag{2}$$

where k_{ij}^{*e} are the element dynamic stiffness coefficients modified by the condensation of the internal degrees of freedom. Subsequently the superscript e is dropped. In the previous equation, the subscript 0 refers to the node on the ffb, whereas n refers to the node on the opposite side of the finite element. In particular, for $n=2$, i.e., for a second order finite element (three-node element),

$$k_{22}^* \;=\; k_{22} \,-\, k_{21}[k_{11}]^{-1}k_{12}$$

$$k_{02}^* \;=\; k_{20}^* \;=\; k_{20} \,-\, k_{21}[k_{11}]^{-1}k_{10} \tag{3}$$

$$k_{00}^* \;=\; k_{00} \,-\, k_{01}[k_{11}]^{-1}k_{10}$$

Hence, the force acting on the ffb is

$$p_0 \;=\; k_{0n}^* u_n \,+\, k_{00}^* u_0 \;=\; k_n u_n \,+\, k_0 u_0 \tag{4}$$

On the other hand, the equilibrium equation for the infinite element, see Fig.2, is

$$p_0^b \;=\; K^b u_0^b \;=\; K u_0^b \tag{5}$$

where $K^b(=K)$ is the infinite element dynamic stiffness matrix. Finally, there must be equilibrium on the ffb, i.e.,

$$p_0 + p_0^b = 0 \tag{6}$$

Compatibility Condition.

Seeking harmonic wave form solutions to Eq.(1), the displacements may be expressed by

$$u(r,\omega t) = Af(\omega t - kr) + Bf(\omega t + kr) = \left(Af(kr) + B\bar{f}(kr)\right)e^{\omega t} \tag{7}$$

where k is the propagation wave number and, $|A|$ and $|B|$ respectively are the amplitudes of the waves traveling in the positive and negative direction of the spatial coordinate r. Note that $\bar{f}(\cdot)$ is the complex conjugate of $f(\cdot)$. The displacements due to waves impinging over and reflected by the ffb, traveling in the adjacent finite element, are expressed by Eq.(7) (for $r_0 \leq r \leq r_0$). The displacements due to waves refracted by the ffb, traveling in the infinite element, are expressed by

$$u^b(r,\omega t) = Cf(kr)e^{\omega t} \tag{8}$$

$(r_0 \leq r)$. Note that $|A|$, $|B|$ and $|C|$ are the amplitudes of the incident, reflected and refracted waves, respectively. On the finite element nodes, Eq.(7) yields

$$u_{0,p} = u(r_{0,p},\omega t) = \left(Af(kr_{0,p}) + B\bar{f}(kr_{0,p})\right)e^{\omega t} = \left(Af_{0,p} + B\bar{f}_{0,p}\right)e^{\omega t} \tag{9}$$

and, on the infinite element node, Eq.(8) yields

$$u_0^b = u^b(r_0,\omega t) = Cf(kr_0)e^{\omega t} = Cf_0 e^{\omega t} \tag{10}$$

Finally, there must be compatibility on the ffb, i.e.,

$$u_0 = u_0^b \tag{11}$$

Therefore, from Eqs.(6) and (11), after using Eqs.(4), (5), (9) and (10), the amplitude ratios are expressed by

$$|B/A| = \sqrt{\frac{\alpha + k_n\beta_1 + \gamma}{\alpha + k_n\beta_2 + \gamma}}$$

$$|C/A| = \frac{|k_n(f_0\bar{f}_n - \bar{f}_0 f_n)/f_0|}{\sqrt{\alpha + k_n\beta_2 + \gamma}}$$

(12)

representing the fraction of the amplitude of the incident wave that is respectively reflected and refracted by ffb. In Eqs.(12),

$$\alpha = \left(|K|^2 + k_0(K+\bar{K}) + (k_0)^2\right)|f_0|^2$$

$$\beta_1 = (\bar{K}+k_0)\bar{f}_0 f_n + (K+k_0)f_0\bar{f}_n$$

$$\beta_2 = (\bar{K}+k_0)f_0\bar{f}_n + (K+k_0)\bar{f}_0 f_n$$

$$\gamma = k_n^2|f_n|^2$$

(13)

In the previous formulae, it has been assumed that the finite elements model undamped media, i.e., k_0 and k_n are real numbers.

Energy Balance.

The mean value of the energy flux passing through the elements is given by

$$<P> = \frac{1}{T} \int_{t_0}^{t_0+T} \text{Re}\{p(\omega t)\}\cdot\text{Re}\{\dot{u}(\omega t)\} \, dt$$

(14)

$(\omega T = 2\pi)$. For harmonic motion,

$$p(\omega t) = pe^{i\omega t}$$

$$u(\omega t) = ue^{i\omega t}$$

(15)

Then, upon integrating Eq.(14),

$$<P> = \frac{1}{4} i\omega(\bar{p}u - p\bar{u})$$

(16)

Hence, by replacing into the equation above, the corresponding expressions for the incident, reflected and refracted waves, from Eqs.(4), (5), (9) and (10), the following mean energy flux values are

obtained

$$<P_A> = \frac{1}{4} i \omega k_n (f_0 \bar{f}_n - \bar{f}_0 f_n)|A|^2$$

$$<P_B> = -\frac{1}{4} i \omega k_n (f_0 \bar{f}_n - \bar{f}_0 f_n)|B|^2 \qquad (17)$$

$$<P_C> = -\frac{1}{4} i \omega (K - \bar{K})|f_0|^2 |C|^2$$

Introducing Eqs.(12) into the equations above, it is easy to prove that the total mean energy flux on the node located over the ffb vanishes, i.e.,

$$<P_A> + <P_B> + <P_C> = 0 \qquad (18)$$

The mean energy flux ratios are

$$<P_B>/<P_A> = -|B/A|^2$$

$$<P_C>/<P_A> = -\frac{(K-\bar{K})|f_0|^2}{k_n(f_0 \bar{f}_n - \bar{f}_0 f_n)}|C/A|^2 \qquad (19)$$

representing the fraction of energy of the incident wave that is respectively reflected and refracted by the ffb.

FINITE ELEMENT APPROXIMATION AND WAVE FORM SOLUTION

Element Characteristic Matrices.

Using classical finite element techniques,[9] the dynamic stiffness matrices may be derived. In particular, the dynamic stiffness matrices of first and second order finite elements may be obtained in closed form. Avoiding the details of a formal derivation, the dynamic stiffness matrices for one-dimensional, cylindrically symmetric, and spherically symmetric elements are shown in Table 1. On the other hand, the corresponding infinite element dynamic stiffness matrices, shown in Table 2, are obtained elsewhere.[4,10,11] For the cylindrically and spherically symmetric cases[11] three wave shape

functions have been assumed: (a) one derived from the exact solution to the wave propagation problem considered; (b) another derived from the asymptotic solution; and (c) the last one assuming an exponential decay. These three cases have been studied to assess the capacity of the infinite elements to transmit the incoming waves into the f, even for the cases when the shape functions are somewhat arbitrarily selected. If only case (a) were treated, spurious reflections would not be produced by the infinite element approximation, since a shape form selected from an exact solution leads to exact results.[10,11]

Wave Propagation Solution.

The harmonic solution to one-dimensional, cylindrically symmetric, and spherically symmetric wave propagation is given[12] by exponential functions, Hankel functions, and spherical Hankel functions, respectively, i.e.,

$$f = \begin{cases} e^{-ikx} \\ H_0^{(2)}(kr) \\ h_1^{(2)}(kR) \end{cases} \qquad \bar{f} = \begin{cases} e^{ikx} \\ H_0^{(1)}(kr) \\ h_1^{(1)}(kR) \end{cases} \tag{20}$$

where $H_0^{(1,2)}$ and $h_1^{(1,2)}$ are the Hankel functions of zero order and the spherical Hankel functions of first order, respectively.

Reflection and Refraction Ratios.

After introducing the equations given in Tables 1 and 2, and Eqs.(20) into Eqs.(12), (13) and (19) the amplitude and mean energy flux ratios may be explicitly obtained for first and second order elements. In the sake of brevity, only the case of one-dimensional wave propagation is given herein. For this case, the amplitude ratios are

$$|B/A|^{m,m^b} = \sqrt{\frac{\mu_1^2 + (\eta^b + \mu_2)^2}{\mu_1^2 + (\eta^b - \mu_2)^2}}$$

$$|C/A|^{m,m^b} = \frac{2|\mu_2|}{\sqrt{\mu_1^2 + (\eta^b - \mu_2)^2}} \tag{21}$$

and the mean energy flux ratios are

$$\{<P_B>/<P_A>\}^{m,m^b} = -\left(|B/A|^{m,m^b}\right)^2$$

(22)

$$\{<P_C>/<P_A>\}^{m,m^b} = \frac{\eta^b}{\mu_2}\left(|C/A|^{m,m^b}\right)^2$$

where

$$\mu_1 = \alpha_0 + \alpha_n\cos\eta$$

$$\mu_2 = \alpha_n\sin\eta$$

(23)

$$\eta^b = \frac{3-m^b}{2}\eta$$

with

$$\alpha_0 = k_0\frac{h}{A_0} = 1 - \frac{3-m}{6}\eta^2$$

(24)

$$\alpha_n = k_n\frac{h}{A_0} = -1 - \frac{m}{6}\eta^2$$

for the first order finite element ($n=1$), and

$$\alpha_0 = k_0\frac{h}{A_0} = \frac{240 - 2(55-3m)\eta^2 + (5-2m)\eta^4}{6(40 - (5-m)\eta^2)}$$

(25)

$$\alpha_n = k_n\frac{h}{A_0} = -\frac{240 + 2(5+3m)\eta^2 + m\eta^4}{6(40 - (5-m)\eta^2)}$$

for the second order finite element ($n=2$). In the preceding equations A_0 is the area disturbed by the traveling wave, and

$$\eta = kh = \frac{2\pi}{\lambda/h}$$

(26)

where h is the element size and λ is the wavelength. The ratio λ/h, number of elements per wavelength, is defined as the *nf* discretization ratio. The parameter m is equal to 1 if the *nf* mass is consistent and equal to 0 if the mass is lumped. Similarly, the parameter m^b refers to the *ff* mass discretization.

NUMERICAL RESULTS

The waves coming from the nf should not be reflected by the ffb. Therefore, the energy and the amplitude of the reflected wave should vanish, i.e., $\{<P_B>/<P_A>\}^{m,m^b}$ and $|B/A|^{m,m^b}$ should be zero. This is equivalent to say that the energy and amplitude of the incident wave is conserved by the refracted wave, i.e., $\{<P_C>/<P_A>\}^{m,m^b} = 1$ and $|C/A|^{m,m^b} = 1$. This occurs only for large values of the discretization ratio, when the mass of the ff is discretized consistently ($m^b=1$), as it may be observed in Fig.3a-d, where the amplitude and mean energy flux ratios are plotted as functions of the discretization ratio. The numerical reflection for low values of the discretization ratio is caused by the different displacement approximations on each side of the ffb. This numerical source of error is diminished by improving the nf displacement approximation.

Reflection-Refraction Levels.
The reflection-refraction level associated to the amplitude is defined as

$$\varepsilon_A^{m,m^b} = \max\left(\left|1-|C/A|^{m,m^b}\right|, |B/A|^{m,m^b}\right) \tag{27}$$

On the other hand, the reflection-refraction level associated to the mean energy flux ratio is defined as

$$\varepsilon_P^{m,m^b} = \max\left(\left|1+\{<P_C>/<P_A>\}^{m,m^b}\right|, \left|\{<P_B>/<P_A>\}^{m,m^b}\right|\right) \tag{28}$$

Furthermore, the reflection-refraction level may be considered acceptable, if it is below 10%; small, if it is below 5%; and negligible, if it is below 1%. On the other hand, for ff consistent mass discretization, the effect of assuming consistent or lumped mass in the nf may be considered very small when the difference between the corresponding reflection-refraction levels is below 2% ($|\varepsilon^{1,1}-\varepsilon^{0,1}|<2\%$).

One-Dimensional Case.
Figures 3a and 3b show the amplitude ratios, for the cases using first and second order elements, respectively. In Figs.3a and 3b the following is observed:

1. $|B/A|^{m,m^b}$ approaches $|1-m^b|/|5-m^b|$ and $|C/A|^{m,m^b}$ approaches $4/|5-m^b|$ when the discretization ratio increases.

2. $|B/A|^{m,m^b}$ approaches 1 when the discretization ratio approaches zero, and $|C/A|^{m,m^b}$ vanishes for discretization ratios equal to $2/j$ $(j=1,2,...)$.

3. In general, for discretization ratios $\lambda/h>2$,

$$\left| |B/A|^{0,m^b} - |1-m^b|/|5-m^b| \right| > \left| |B/A|^{1,m^b} - |1-m^b|/|5-m^b| \right| > 0 \qquad \text{and}$$

$$\left| |C/A|^{0,m^b} - 4/|5-m^b| \right| > \left| |C/A|^{1,m^b} - 4/|5-m^b| \right| > 0. \text{ For second order elements, the first}$$

relationship is not valid in the neighborhood of $\lambda/h=2.34$, when the ff is modeled with lumped mass. The second relationship is not valid in the neighborhood of $\lambda/h=2.07$ for any model of ff.

Figures 3c and 3d show the mean energy flux ratios, for the cases using first and second order elements, respectively. In Figs.3c and 3d the following is observed:

1. $\{<P_B>/<P_A>\}^{m,m^b}$ approaches $-(1-m^b)^2/(5-m^b)^2$ and $\{<P_C>/<P_A>\}^{m,m^b}$ approaches $-8(3-m^b)/(5-m^b)^2$ when the discretization ratio increases.

2. $\{<P_B>/<P_A>\}^{m,m^b}$ approaches -1 when the discretization ratio approaches zero, and $\{<P_C>/<P_A>\}^{m,m^b}$ vanishes for discretization ratios equal to $2/j$ $(j=1,2,...)$.

3. In general, for discretization ratios $\lambda/h>2$,

$$\left| \{<P_B>/<P_A>\}^{0,m^b} + (1-m^b)^2/(5-m^b)^2 \right| > \left| \{<P_B>/<P_A>\}^{1,m^b} + (1-m^b)^2/(5-m^b)^2 \right| > 0 \qquad \text{and}$$

$$\left| \{<P_C>/<P_A>\}^{0,m^b} + 8(3-m^b)/(5-m^b)^2 \right| > \left| \{<P_C>/<P_A>\}^{1,m^b} + 8(3-m^b)/(5-m^b)^2 \right| > 0. \qquad \text{For}$$

second order elements, these relationships are not valid in the neighborhood of $\lambda/h=2.34$, when the ff is modeled with lumped mass.

Note that when the ff mass is lumped the reflected wave does not vanish as the discretization ratio becomes large. In effect,

$$\varepsilon_A^{m,b}(\lambda/h \rightarrow \infty) = 20\%$$

$$\varepsilon_P^{m,b}(\lambda/h \rightarrow \infty) = 4\%$$

(29)

Hence, lumping the ff mass generates waves being reflected by the ffb which leads to spurious results. The amplitude of this reflected wave is at least 20% of the amplitude of the incident wave, and the mean energy flux carried by this wave back into the nf is at least 4% of the mean energy flux carried by the incident wave.

Polar and Spherical Symmetry.

In progress.

ANALYSIS OF THE RESULTS

General Remarks.

The errors caused by the artificial scattering effect due to a finite/infinite element discretization of a semi-infinite region are studied. Two obvious results are numerically verified: (a) the larger the number of elements per wavelength, the smaller the reflections; and (b) the higher the order of the numerical displacement approximation, the smaller the reflections. The artificial reflections on the ffb depend on the nf discretization. If the ff displacement approximation is not exact, the errors due to the artificial reflections on the ffb would increase. No attempt is made to try different ff displacement approximations, since, for the case of one-dimensional wave propagation, the ff solution can be obtained analytically and then applied to any suitable numerical procedure. If the discretization ratio varies in the nf, another source of error is introduced.[6,7]

The discrepancies in the results between elements of first and second order are significant for low values of the discretization ratio. It is also observed that using lumped mass in the nf, as opposed to consistent mass, leads to significant errors for low values of the discretization ratio. However, when lumping the mass in the ff, the errors become large and do not vanish, even when the discretization ratio increases.

Recommendations.

From the numerical results shown, it is possible to obtain criteria for rational mesh design, in order to diminish numerical reflections produced by artificial boundaries, when treating transient and wave propagation problems defined in unbounded media. By using an exact ff displacement approximation, the source of error is restricted to the nf. Then, the nf must be discretized in elements such that the ratio between the shortest wavelength and the longest element is larger than or equal to a critical discretization ratio, i.e.,

$$\frac{\lambda_{min}}{h_{max}} = \frac{2\pi}{\omega_{max}h_{max}} \geq (\lambda/h)_{cr} \tag{30}$$

where ω_{max} is the cut-off frequency corresponding to the shortest wavelength, λ_{min}, and h_{max} is the size of the longest element present in the nf discretization. As critical discretization ratio it is understood by the discretization ratio giving the maximum allowable reflection-refraction level.

Then, the critical discretization ratios for acceptable, small and negligible reflection-refraction levels may be obtained directly from Table 3, where it can also be obtained the critical discretization ratio above which the effect of the nf mass discretization is very small. In Table 3, it can be seen that the second order element provides a good solution from the standpoint of the model accuracy and of the critical discretization ratio needed to yield that accuracy. It is clearly disadvantageous to lump the nf mass for critical discretization ratios, if a small level of reflection-refraction is required. To reach below the same reflection-refraction levels as reached when using consistent mass in the nf, it is necessary to use larger discretization ratios for lumped mass, leading to a larger number of degrees of freedom per wavelength.

CONCLUSIONS

To discretize an unbounded medium for analyzing transient and wave propagation problems it is necessary to lend attention to the size of the near-field discretization with respect to the wavelength (of the waves necessary to include in the solution). The finite element (or finite difference) numerical model should be able to numerically propagate the corresponding waves without introducing spurious reflections coming from artificial boundaries. Considering one-dimensional wave propagation, it is numerically determined that the critical discretization ratio $(\lambda/h)_{cr}$ is equal to 3.7 for first order elements and 2.1 for second order elements. With these critical discretization ratios it is secured that the reflections coming from the numerical model are acceptable (smaller than 10%). In the case of the second order element the reflection level is around 5%. Lumping the mass in the near field leads to large reflections, whereas lumping the mass in the far field leads to unacceptable results.

ACKNOWLEDGEMENTS

REFERENCES

1. R.F. Ungless, 'An Infinite Finite Element,' *M.A.Sc.thesis*, U.British Columbia (1973).

2. P. Bettess, 'Infinite Elements,' *Int.J.num.Meth.Engng.*, 11,53-64(1977).

3. P.Bettess and O.C.Zienkiewicz, 'Diffraction and Refraction of Surface Waves Using Finite and Infinite Elements,' *Int.J.num.Meth.Engng.*, 11,1271-1290(1977).

4. F. Medina, 'Modelling of Soil-Structure Interaction by Finite and Infinite Elements,' *rep. UCB/EERC-80/43*, U.California, Berkeley (1980).

5. Y.K. Chow, and I.M. Smith, 'Static and Periodic Infinite Solid Elements,' *Int.J.num.Meth. Engng.*, 17,503,526(1981).

6. Z. Bažant, 'Spurious Reflection of Elastic Waves in Nonuniform Finite Element Grids,' *Comp. Meth.Appl.Mech.Engng.*, 16,91-100(1978).

7. Z. Bažant and Z. Celep, 'Spurious Reflection of Elastic Waves in Nonuniform Meshes of Constant and Linear Strain Finite Elements,' *Comp.&Struct.*, 15,451-459(1982).

8. W.C. Hurty and M.F. Rubinstein, *Dynamics of Structures*, Prentice-Hall (1964).

9. O.C. Zienkiewicz, *The Finite Element Method*, 3rd ed McGraw-Hill (1978).

10. F. Medina and F. Rosales, 'Spurious Reflections and Accuracy of Finite Element Models for Unbounded Wave Propagation Problems: The One-Dimensional Case,' *Engng.Comp.*, 4,137-148(1988).

11. F. Medina and F. Rosales, 'Spurious Reflections and Accuracy of Finite Element Models for Unbounded Wave Propagation Problems: The Two- and Three-Dimensional Cases,' to be submitted to the *Int.J.num.Meth.Engng.* (1988).

12. K.F. Graff, *Wave Motion in Elastic Solids*, Ohio State Univ. Press (1975).

Table 1.- Finite element dynamic stiffness matrices, K^e.

ONE-DIMENSIONAL CASE:

2-node element

$$\frac{A_0}{h}\left[-\frac{\eta^2}{6}\begin{bmatrix}3-m & m \\ m & 3-m\end{bmatrix} + \begin{bmatrix}1 & -1 \\ -1 & 1\end{bmatrix}\right]$$

3-node element

$$\frac{A_0}{h}\left[-\frac{\eta^2}{30}\begin{bmatrix}5-m & 2m & -m \\ 2m & 20-4m & 2m \\ -m & 2m & 5-m\end{bmatrix} + \frac{1}{3}\begin{bmatrix}7 & -8 & 1 \\ -8 & 16 & -8 \\ 1 & -8 & 7\end{bmatrix}\right]$$

CYLINDRICAL SYMMETRY:

2-node element

$$2\pi b\left[-\frac{\eta^2}{12}\begin{bmatrix}2(3-m)\bar\rho-1 & 2m\bar\rho \\ 2m\bar\rho & 2(3-m)\bar\rho+1\end{bmatrix} + \bar\rho\begin{bmatrix}1 & -1 \\ -1 & 1\end{bmatrix}\right]$$

3-node element

$$2\pi b\left[-\frac{\eta^2}{60}\begin{bmatrix}2(5-m)\bar\rho-5+2m & 2m(2\bar\rho-1) & -2m\bar\rho \\ 2m(2\rho-1) & 8(5-m)\bar\rho & 2m(2\bar\rho+1) \\ -2m\bar\rho & 2m(2\bar\rho+1) & 2(5-m)\bar\rho+5-2m\end{bmatrix} + \frac{1}{3}\begin{bmatrix}7\bar\rho-2 & -8\bar\rho+2 & \bar\rho \\ -8\bar\rho+2 & 16\bar\rho & -8\bar\rho-2 \\ \bar\rho & -8\bar\rho-2 & 7\bar\rho+2\end{bmatrix}\right]$$

SPHERICAL SYMMETRY:

2-node element

$$\pi h\left[-\frac{\eta^2}{30}\begin{bmatrix}20(3-m)\bar P^2-20\bar P+5-m & (20\bar P^2+1)m \\ (20\bar P^2+1)m & 20(3-m)\bar P^2+20\bar P+5-m\end{bmatrix} + \begin{bmatrix}4\bar P^2+3 & -4\bar P^2+1 \\ -4\bar P^2+1 & 4\bar P^2+3\end{bmatrix}\right]$$

3-node element

$$-\frac{\pi h\eta^2}{210}\begin{bmatrix}28(5-m)\bar P^2-28(5-2m)\bar P+3(7-m) & (56\bar P^2-56\bar P+6)m & -(28\bar P^2+3)m \\ (56\bar P^2-56\bar P+6)m & 112(5-m)\bar P^2+4(7-3m) & (56\bar P^2+56\bar P+6)m \\ -(28P^2+3)m & (56\bar P^2+56\bar P+6)m & 28(5-m)\bar P^2+28(5-2m)\bar P+3(7-m)\end{bmatrix} +$$

$$+ \frac{\pi h}{15}\begin{bmatrix}140\bar P^2-80\bar P+33 & -16(10\bar P^2-5\bar P+1) & 20\bar P^2+3 \\ -16(10\bar P^2-5\bar P+1) & 16(20\bar P^2+7) & -16(10\bar P^2+5\bar P+1) \\ 20\bar P^2+3 & -16(10\bar P^2+5\bar P+1) & 140\bar P^2+80\bar P+33\end{bmatrix}$$

PARAMETER DEFINITIONS:

η = kh = $\omega h/c$, dimensionless wave number.

k = $2\pi/\lambda$, wave number.

λ = wavelength.

h = element size.

c = wave propagation velocity.

A_0 = area disturbed by the one-dimensional wave propagation.

b = thickness disturbed by the polar wave propagation.

m = mass parameter (=1, consistent mass; =0, lumped mass).

$\bar\rho$ = $\bar r/h$, $\bar P$ = $\bar R/h$

$\bar r$ = $(r_0+r_n)/2$, $\bar R$ = $(R_0+R_n)/2$

r = $\sqrt{x^2+y^2}$, R = $\sqrt{\bar r^2+\bar y^2}$

Table 2.- Infinite element dynamic stiffness matrices, K^b.

SHAPE FUNCTION	ONE-DIMENSIONAL	POLAR SYMMETRY	SPHERICAL SYMMETRY
EXACT	$\dfrac{3-m^b}{2}ikA_0$	$2\pi b\; k_0\dfrac{H_1^{(2)}(k_0)}{H_0^{(2)}(k_0)}$	$4\pi R_0\left(2 - K_0\dfrac{h_0^{(2)}(K_0)}{h_1^{(2)}(K_0)}\right)$
ASYMPTOTIC		$\pi b\left(1/2 + ik_0(2+I(k_0))\right)$	$4\pi R_0\left(3 + iK_0(1-4I(K_0))\right)$
EXPONENTIAL		$\pi b\dfrac{3 - 10k_0^2 + i4k_0(2-k_0^2)}{2(1 + ik_0)^2}$	$\pi R_0\dfrac{9 - 28K_0^2 + 4K_0^4 + i8K_0(3-2K_0^2)}{(1 + iK_0)^3}$

- PARAMETER DEFINITIONS:

m^b = mass parameter (=1, consistent mass; =0, lumped mass).

k_0 = kr_0, polar dimensionless wave number.

K_0 = kR_0, spherical dimensionless wave number.

r_0, R_0 = infinite element nodal coordinates.

$H_n^{(2)}$ = Hankel function of the second kind and order n.

$h_n^{(2)}$ = spherical Hankel function of the second kind and order n.

$I(r)$ = $\displaystyle\int_0^\infty \frac{e^{-i2rt}}{1+t}dt$ = $e^{i2r}\cdot E_1(i2r)$.

E_1 = exponential-integral function.

Others, as indicated in Table 1.

Table 3.- Minimum discretization ratios (λ/h) for different error levels in the computation of the numerical scattering on the far-field boundary of a semi-infinite rod.						
ELEMENT ORDER	$\epsilon^{m,j} \leq 10\%$		$\epsilon^{m,j} \leq 5\%$		$\epsilon^{m,j} \leq 1\%$		$|\epsilon^{1,j} - \epsilon^{0,j}| \leq$
	m=1	m=0	m=1	m=0	m=1	m=0	
FIRST:							
$- \epsilon_A^{m,j}$	3.72	5.95	4.67	8.27	8.00	18.22	12.70
$- \epsilon_P^{m,j}$	2.63	3.54	2.90	4.12	3.72	5.95	4.97
SECOND:							
$- \epsilon_A^{m,j}$	2.06	2.66	2.16	2.92	3.17	3.82	3.23
$- \epsilon_P^{m,j}$	2.02	2.37	2.03	2.44	2.06	2.66	2.55

(a)

(b)

(c)
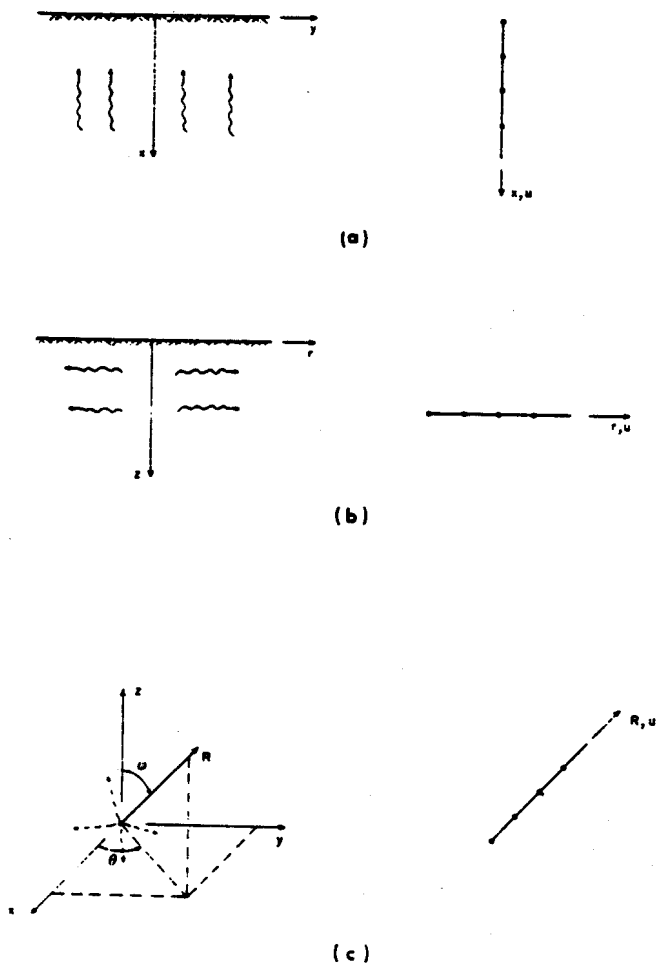
Figure 1.- Wave propagation problems discretized in one-dimension. (a) One-dimensional case. (b) Cylindrical symmetry. (c) Spherical symmetry.
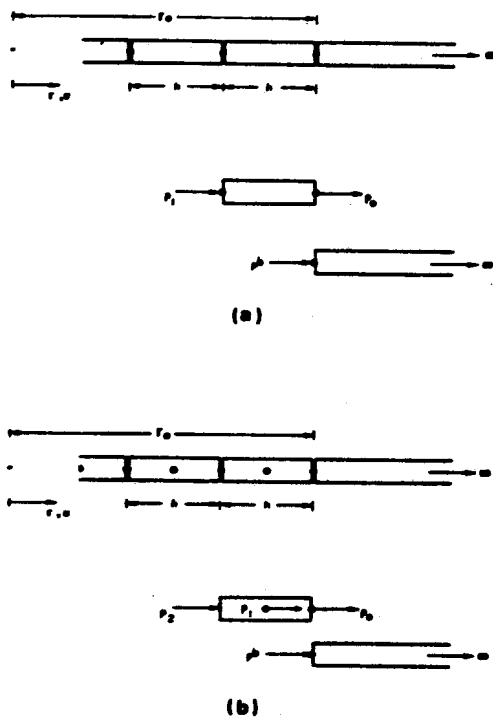
Figure 2.- Models to compute the numerical reflections produced on the far-field boundary. (a) Geometry for the case of first order finite elements. (b) Geometry for the case of second order finite elements.
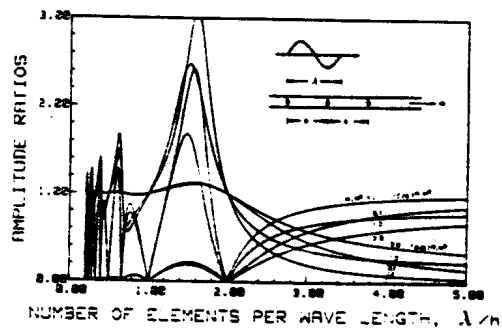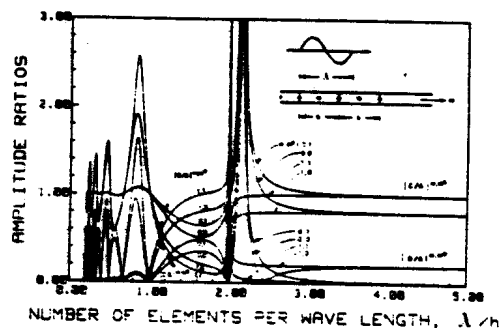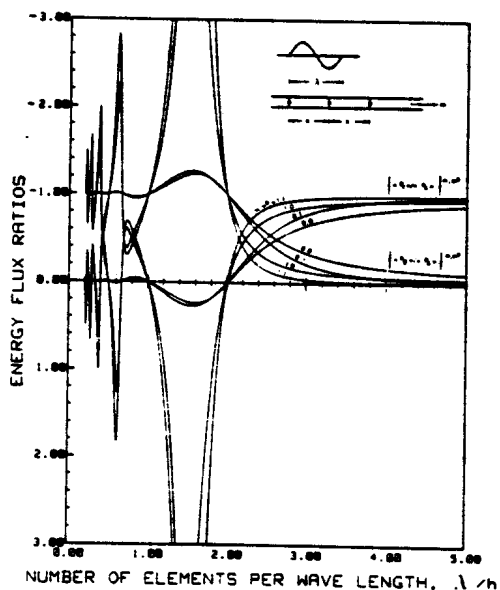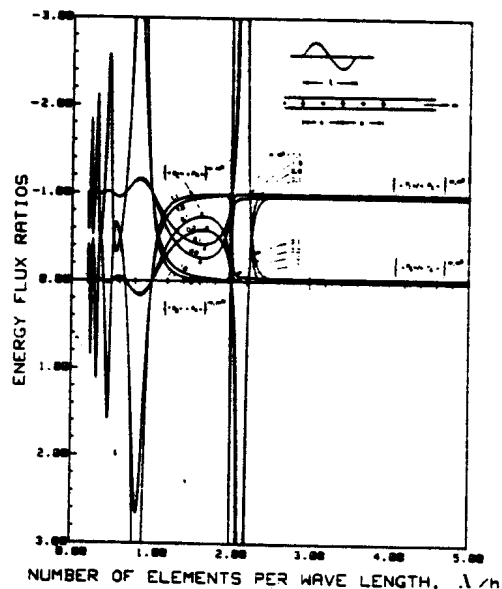
Figure 3.- Computation of numerical scattering produced on the far-field boundary by means of amplitude and mean energy flux ratios between reflected and incident waves and between refracted and incident waves. (a) Amplitude ratio for models using first order finite elements. (b) Amplitude ratio for models using second order finite elements. (c) Mean flux ratio for models using first order finite elements. (d) Mean flux ratio for models using second order finite elements.